

Tumor Metastasis Simulation via Lattice-Gas Cellular Automata

Abstract

Cancer remains a devastating disease even in the modern era of medicine. While the molecular characteristics of cancer growth have been studied for some time, it is only relatively recently that methods within computational biology have been applied to this aspect of oncology. As computational capabilities progress, tumor growth may prove to be pragmatically studied *in silico*. One such method study leverages the conceptual foundation of the cellular automata model and extends it using physical concepts, including the Cellular Potts model and gaseous fluid theory as applied to Euclidean lattices of cells.

Purpose: Implementation of a cellular automata model that is modular with respect to neighborhoods, dimensions, plotting, and physical constants.

§1. Introduction

This cellular automata simulation leverages existing models first developed to simulate gaseous particles and applies the same computational logic to growing tumor cells. The so-called Lattice Gas Cellular Automata (LGCA) uses a finite Euclidean lattice of cell “sites”, such that each site has interactivity with neighboring sites via predefined neighborhood bounds (Von Neumann; this particular choice is further explained). Additionally, proxies for cell-to-cell interaction *within* neighborhoods are modeled via like-type proximity. This approach was first implemented computationally and plotted in two dimensions, and then implemented in three dimensions.

§2. Methods

§2.1 Two-Dimensional LGCA

Lattice-Gas Cellular Automata (in two dimensions) leverages existing principles of cellular automata¹ and adds movement of particles – cells with states this case – through discrete velocity vectors on a two-dimensional matrix. Depending on its local Von Neumann neighborhood, a given cell’s likely state in the next timestep of the simulation is computed (the “reactive step”). Then, a cell’s propensity to move or propagate is applied via stochastic movement along discrete vectors to neighboring sites (Von Neumann neighborhoods, whereby each site on the lattice is associated with five possible channels of movement).

To this end, we wrote a *Go* program that declares a two-dimensional lattice of cell structs, whereby each cell bears a state in the form of a string, a location in the form of an ordered pair of integers, a velocity direction (for movement and propagation purposes), and an array of pointers to cells of its local neighborhood.

§2.2 Reactive Step

Cells may transition from state to state²³. That is, we define “cells” within the lattice as either cancerous, healthy, or necrotic. Cancerous cells can either be in a state of quiescence (non-propagative, but not necrotic either) or in a proliferative state (whereby cell division will take place and a new cancer cell will propagate at the next timestep). Necrotic cells are defined as previously

¹ Stephen Wolfram, “Statistical Mechanics of Cellular Automata,” *Reviews of Modern Physics* 55, no. 3 (July 1, 1983): 601–44, <https://doi.org/10.1103/RevModPhys.55.601>.

² This simulation has roots in the Ising Model of ferromagnetic dipole moments as applied to the Glauber Algorithm, except here we consider +1 and -1 spin states as proportional to cancerous or necrotic cells.

³ “Glauber’s Dynamics | Bit-Player,” accessed November 29, 2019, <http://bit-player.org/2019/glaubers-dynamics>.

cancerous cells that died due to lack of available resources (space, in this case). Healthy cells are simulated as sites on the lattice not occupied by other cells, or sites upon which other cells can invade and spread. Apoptotic cells were additionally modeled though not implemented in the runnable simulation for simplicity, though modular, workable code is included as “commented” code.

Cell state transitions are computed probabilistically via a simplified adaptation of Lattice-Boltzmann Energy theory. Three cell coupling coefficient⁴ parameters are employed to this effect: K_{cc} , K_{nn} , and K_{cn} . These represent modeling constants proportional to the strength of membrane coupling between cancer cells (quiescent included), necrotic-necrotic cell interaction, and cancerous-necrotic interaction.

Next, these constants are imputed into Lattice-Boltzmann energy factor equations defined for cells of type proliferative, quiescent, and necrotic, together with the count of cells of each type in the current neighborhood (C , N , for cancerous and necrotic, respectively):

1. $E_p = -[0.50(C(C + 1)) K_{cc} + N(N - 1)K_{nn}] + (C + 1)N K_{cn}]$
2. $E_q = -[0.50((C - 1)(C)) K_{cc} + N(N - 1)K_{nn}] + (C)N K_{cn}]$
3. $E_n = -[0.50((C - 1)(C - 2)) K_{cc} + N(N + 1)K_{nn}] + (C - 1)(N + 1) K_{cn}]$

⁴ Dieter A. Wolf-Gladrow, *Lattice-Gas Cellular Automata and Lattice Boltzmann Models An Introduction*, 1st ed. 2000., Lecture Notes in Mathematics, 1725 (Berlin, Heidelberg: Springer Berlin Heidelberg, 2000), <https://doi.org/10.1007/b72010>.

In other words, one of the following reactions is possible for between any two given timesteps at site i, j of the lattice ⁵:

4. Proliferation: $C_{i,j} \rightarrow C_{i,j} + 1 ; N_{i,j} \rightarrow N_{i,j} .$
5. Quiescence: $C_{i,j} \rightarrow C_{i,j} ; N_{i,j} \rightarrow N_{i,j}$ (no change).
6. Necrosis: $C_{i,j} \rightarrow C_{i,j} - 1 ; N_{i,j} \rightarrow N_{i,j} + 1 .$

Note that these Boltzmann models are highly related, proportional abstractions of the Hamiltonian energy model employed in the generalized Cellular Potts⁶ automata model⁷.

Next, these computed Boltzmann energies are imputed into a simplified^{8,9} lattice-gas probability model, such that proxies for proliferative, quiescence, and necrosis likelihoods are obtained by comparing ratios of Boltzmann factors¹⁰:

⁵ Mehrdad Ghaemi and Amene Shahrokhi, “Combination of the Cellular Potts Model and Lattice Gas Cellular Automata for Simulating the Avascular Cancer Growth,” in *Cellular Automata*, ed. Samira El Yacoubi, Bastien Chopard, and Stefania Bandini (Berlin, Heidelberg: Springer Berlin Heidelberg, 2006), 297–303.

⁶ null Graner and null Glazier, “Simulation of Biological Cell Sorting Using a Two-Dimensional Extended Potts Model,” *Physical Review Letters* 69, no. 13 (September 28, 1992): 2013–16, <https://doi.org/10.1103/PhysRevLett.69.2013>.

⁷ That is, $E_x \propto H = \sum_{Neighbors(x_{i,j})} J \left(\tau(\sigma_i), \tau(\sigma_j) \right) \left(1 - \delta(\sigma_i, \sigma_j) \right) + \lambda \sum_i \left(v(\sigma_i) - V(\sigma_i) \right)^2$, where i, j are lattice sites, J is the boundary coefficient determining the adhesion between two cells of types $\tau(\sigma), \tau(\sigma')$ (C, N in the current model), σ_i is the cell at site i , $\tau(\sigma)$ is the cell type of cell σ , J is a boundary coefficient determining the adhesion between two cells of types $\tau(\sigma), \tau(\sigma')$, δ is the Kronecker Delta, $v(\sigma)$ the volume (area in two dimensions) function, $V(\sigma)$ the target volume (area in two dimensions, but not applicable to the current model since spatial constraints per neighborhood are implicitly enforced), and λ a Lagrange multiplier to determine the optimized strength of the volume constraint.

⁸ Boltzmann factors as defined in literature are simplified in this model to ensure no 64-bit floating point issues given the magnitude of the constants involved. That is, $e^{\frac{-\Delta E_x}{kT}} \propto e^{E_x}$, where x is cell state.

⁹ Barry Doyle et al., eds., *Computational Biomechanics for Medicine* (New York, NY: Springer New York, 2014), chap. 2, <https://doi.org/10.1007/978-1-4939-0745-8>.

¹⁰ Note that these computational steps are highly modular. Additional cell types and constraints are easily implemented at the level of code if desired.

$$7. P_{proliferative} = \frac{e^{E_p}}{e^{E_p} + e^{E_q} + e^{E_n}}$$

$$8. P_{quiescent} = \frac{e^{E_q}}{e^{E_p} + e^{E_q} + e^{E_n}}$$

$$9. P_{necrosis} = \frac{e^{E_n}}{e^{E_p} + e^{E_q} + e^{E_n}}$$

States of each cell on the lattice are then updated according to these probabilities at each timestep.

§2.3 Movement Step

Following the computational “reactive step” above, each cell is primed for potential movement as a function of their probabilistic states. Propagative cancerous cells will divide, with nascent cells invading the adjacent neighborhood least dense in cancerous cells (modeling invasion), with parental cells remaining in a current site. Modeling principles of chemotaxis¹¹, necrotic cells will move toward regions *most* dense in other necrotic cells (the simulation plots a path of movement). Finally, quiescent cancer cells will not move. If a tie is obtained between cell-type densities in adjacent neighborhoods (e.g., if two or more adjacent neighborhoods contain the same number of *C* or *N* cells), one of these equivalent neighborhoods is chosen at random for cell movement and/or propagation.

Cells of relevant types are then moved synchronously (i.e., a single timestep change results in all cells updated across the lattice and within neighborhoods) at the given timestep, resulting in an

¹¹ Evanthia T. Roussos, John S. Condeelis, and Antonia Patsialou, “Chemotaxis in Cancer,” *Nature Reviews. Cancer* 11, no. 8 (July 22, 2011): 573–87, <https://doi.org/10.1038/nrc3078>.

updated lattice. Note that a Von Neumann cellular automata neighborhood (see Figure 1.) was chosen in this instance due to practicality of implementation¹² as well as reasons of physical verisimilitude¹³.

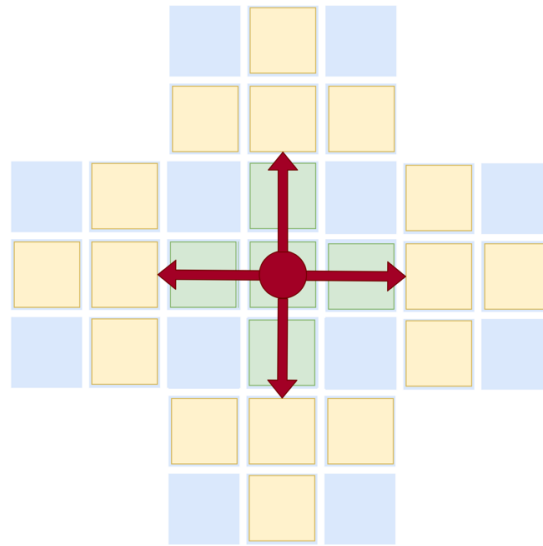


Figure 1. 2-D Von Neumann neighborhood with adjacent lattice sites. Velocity vectors superimposed.

§2.4 Plotting

§2.5 Beyond 2 Dimensions

The implementation of this simulation is highly modular, and the code easily lends itself to expansion. One such expansion that was implemented was an extension to three-dimensional

¹² A Von Neumann cellular automata neighborhood was chosen in this instance mainly due to memory constraints. An original implementation for this project used a strictly three-dimensional Moore neighborhood, for a total of 26 neighbors. Since we aimed to preserve prior lattice states for plotting, this quickly became impractical when computing on local machines.

Additionally, a square or cubic Von-Neumann neighborhood (in two or three dimensions) obeys the Platonic solid principle, such that lattice vectors are all of equal length (an important assumption imputed into the cell behavior). Other Platonic-solid neighborhoods include octahedral, dodecahedral, and icosahedral adjacency vectors (the modularity of this model would easily allow a future implementation to make use of these more complex neighborhoods).

¹³ Wolf-Gladrow, *Lattice-Gas Cellular Automata and Lattice Boltzmann Models An Introduction*, 106.

space. That is, a three-dimensional lattice of cells were defined on a row, column, and “aisle” basis. All computational and logistical two-dimensional functions were then altered to accommodate the new spatial arrangement of the simulation.

§2.6 Three-Dimensional Reactive Step

This step is logically equivalent to that of the two-dimensional implementation (see §2.2), only that cell states at a given timestep are defined by a three-dimensional Von Neumann neighborhood (see Figure 2.)

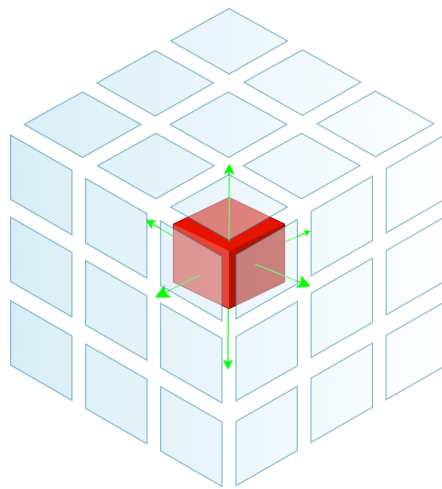


Figure 2. The 3-D Von Neumann arrangement, with velocity vectors of the center cell superimposed.

§2.7 Propagation Step in Three Dimensions

Cell movement and propagation is again equivalent logically to the two-dimensional implementation (see §2.3), only that the implementation required an extension into the “aisle” space, accommodating the extra dimension. Cell movement has two extra potential axes (see Figure 2.) for two additional discrete velocity vectors.

§2.8 Plotting in Three Dimensions

§3. Results

§3.1 Two-Dimensional Plot

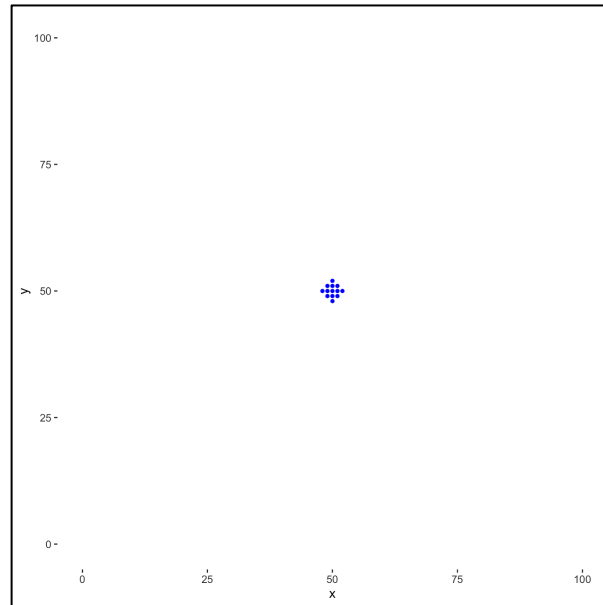


Figure 3. Initial two-dimensional lattice seeded with a cancerous central neighborhood and adjacent sites. Units in cells (pixels).

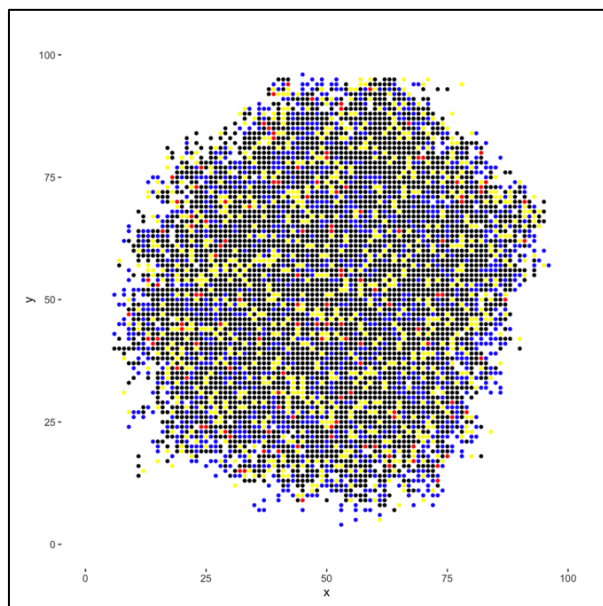


Figure 4. Lattice after 50 generations of growth.

§3.2 Three-Dimensional Plot

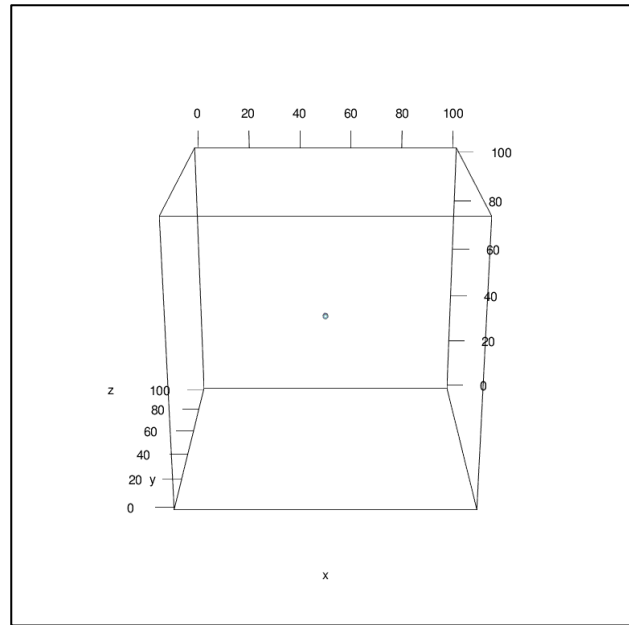


Figure 5. Three-dimensional lattice similarly seeded with cancerous cells.

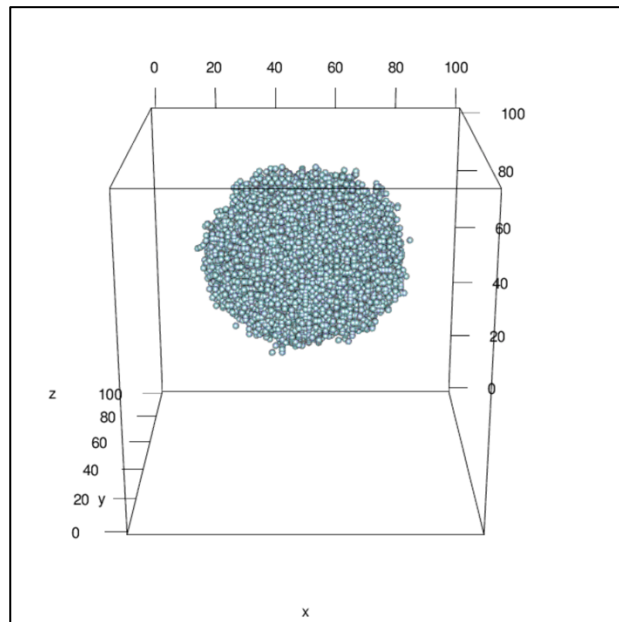


Figure 6. Three-dimensional lattice after 35 generations of the simulation (only cancerous cells plotted for simplicity).

§3.3 Discussion

The model was simulated on a two-dimensional lattice for 50 generations (see Figures 3,4.), and a three-dimensional model was simulated for 35 generations of growth (see Figures 5,6.). Additionally, for this simulation, coupling constant parameters were set to $K_{cc} = K_{nn} = 3.0$; $K_{nc} = 1.0$ per the advice of previous two-dimensional investigation¹⁴.

Though the rules employed in this automata are somewhat simple compared to true cellular dynamics, nonetheless tumor “cells” are modeled somewhat realistically. Competition for resources (spatial constraints) here between healthy (background) cells and proliferative cancer cells is apparent, as is the complex interplay between cells of difference states.

¹⁴ Doyle et al., *Computational Biomechanics for Medicine*, chap. 2.

§4. Conclusions

This implementation represents a successful, novel implementation of lattice-gas cellular automata as applied to principles of tumor growth. Furthermore, this implementation can be run in virtually infinitely many ways simply by altering existing constraints. Additionally, the model is sufficiently modular to allow for simple expansion, such as the addition of apoptotic cells, healthy cell behavior, additional coupling constraints, and more complex neighborhood geometry.

Some limitations of this model are apparent, however. The implementation is compute-intensive and memory-heavy; more complex investigations would need to better utilize principles of parallelism to remain practical. Additionally, it is unclear how a fundamentally bitmap-based model such as this would scale to much larger numbers of cells. Perhaps vector-drawn “cells”, with internal environments, would be apropos in a future implementation.

Future expansion upon this model could additionally incorporate real-time rendering rather than precomputation of lattices for plotting. In *Go*, this is conceivable via rendering into two images at alternate timepoints, and plotting one of them, such that one image is always being “painted” and one displayed. This could be further optimized via use of the additional CPU cores (or a GPU) if local rendering is required.

In conclusion, this model, while simple, is an arguably powerful multifaceted tool for simulating cancerous cell growth *in silico*.

§5. Works Cited

- Doyle, Barry, Karol Miller, Adam Wittek, and Poul M.F. Nielsen, eds. *Computational Biomechanics for Medicine*. New York, NY: Springer New York, 2014. <https://doi.org/10.1007/978-1-4939-0745-8>.
- Ghaemi, Mehrdad, and Amene Shahrokhi. "Combination of the Cellular Potts Model and Lattice Gas Cellular Automata for Simulating the Avascular Cancer Growth." In *Cellular Automata*, edited by Samira El Yacoubi, Bastien Chopard, and Stefania Bandini, 297–303. Berlin, Heidelberg: Springer Berlin Heidelberg, 2006.
- "Glauber's Dynamics | Bit-Player." Accessed November 29, 2019. <http://bit-player.org/2019/glaubers-dynamics>.
- Graner, null, and null Glazier. "Simulation of Biological Cell Sorting Using a Two-Dimensional Extended Potts Model." *Physical Review Letters* 69, no. 13 (September 28, 1992): 2013–16. <https://doi.org/10.1103/PhysRevLett.69.2013>.
- Roussos, Evanthia T., John S. Condeelis, and Antonia Patsialou. "Chemotaxis in Cancer." *Nature Reviews. Cancer* 11, no. 8 (July 22, 2011): 573–87. <https://doi.org/10.1038/nrc3078>.
- Wolf-Gladrow, Dieter A. *Lattice-Gas Cellular Automata and Lattice Boltzmann Models An Introduction*. 1st ed. 2000. Lecture Notes in Mathematics, 1725. Berlin, Heidelberg: Springer Berlin Heidelberg, 2000. <https://doi.org/10.1007/b72010>.
- Wolfram, Stephen. "Statistical Mechanics of Cellular Automata." *Reviews of Modern Physics* 55, no. 3 (July 1, 1983): 601–44. <https://doi.org/10.1103/RevModPhys.55.601>.